

The Partially Observable Hidden Markov Model with Application to Keystroke Biometrics

John V. Monaco, *Member, IEEE*, and Charles C. Tappert



arXiv:1607.03854v3 [cs.IT] 29 Aug 2016

Abstract—This work introduces the partially observable hidden Markov model (POHMM), an extension of the hidden Markov Model (HMM) in which the hidden state emission and transition parameters depend on observed event types that form an independent Markov chain. Despite an explosion in the number of model parameters, parameter estimation can still be performed in time that scales linearly with the number of observations. Marginal distributions of the model act as a fallback mechanism when novel event types are encountered during likelihood estimation. A parameter smoothing technique accounts for missing data during parameter estimation and simultaneously reduces the degrees of freedom of the model to avoid overfitting. The structure of the POHMM is motivated by sequences that contain metadata which may partially reveal the underlying hidden state. Such a scenario is encountered in keystroke biometrics where the user is in either an active or passive state of typing, and the keyboard key names are event types that partially reveal the hidden state. The proposed model is shown to consistently outperform other anomaly detectors, including the standard HMM, in biometric identification and verification tasks and is generally preferred over the HMM in a Monte Carlo goodness of fit test.

Index Terms—hidden Markov model, behavioral biometrics, keystroke dynamics, time intervals

1 INTRODUCTION

TIME interval biometrics utilize the timestamps from a sequence of timed events for the purpose of identification and verification. The time intervals, i.e., the time between events, is of interest. Let t_n be the time of the n^{th} event. The sequence of time intervals is given by

$$\tau_n = t_n - t_{n-1}. \quad (1)$$

In the case an event has duration, t_n marks the time of onset.

There are many scenarios in time interval biometrics in which there is also some metadata, such as an event type, associated with each event. For example, consider a two-state model of typing behavior in which the user can be in either an active or passive state of typing. The keyboard key names can be considered event types that partially

- John V. Monaco is with the Computational and Information Sciences Directorate, U.S. Army Research Laboratory, Aberdeen, MD 21005, USA. E-mail: john.v.monaco2.ctr@mail.mil
- Charles C. Tappert is with the Seidenberg School of Computer Science and Information Systems, Pace University, Pleasantville, NY, 10570.

This research was supported in part by an appointment to the Postgraduate Research Participation Program at the U.S. Army Research Laboratory administered by the Oak Ridge Institute for Science and Education through an interagency agreement between the U.S. Department of Energy and USARL.

reveal the hidden state. The posterior probability of being in either an active or passive state of typing may be greater depending on which key was pressed. Certain keys, such as punctuation and the Space key, may indicate a greater probability of being in a passive state as the typist often pauses between words and sentences as opposed to between letters in a word [25]. This reasoning extends to other activities, such as email, in which a user might be more likely to pause after sending an email instead of receiving an email, and programming, in which a user may fix bugs quicker than making feature additions. In all these examples, the event types, such as keys pressed, characterize what the system is doing, while the observations, such as keystroke timings, characterize how the system behaves.

This work introduces the partially observable hidden Markov model (POHMM), a generalization of the hidden Markov model (HMM) in which the hidden state is conditioned on an event type. The event types are observed and form an independent Markov chain that characterizes some other process, such as a task the system must perform. The hidden states depend on the event types and form a latent Markov chain that characterizes how the system behaves. Despite an explosion in the number of model parameters, parameter estimation can still be performed in time that scales linearly with the number of observations. Marginal distributions of the model act as a fallback mechanism when novel event type sequences are encountered during likelihood estimation. A parameter smoothing technique is used to account for missing data during parameter estimation and simultaneously reduce the degrees of freedom of the model to avoid overfitting.

The rest of this article is organized as follows. Section 2 reviews the standard HMM and defines a two-state HMM for temporal behavior. Section 3 describes the POHMM, followed by a simulation study in Section 4 and a case study of the POHMM applied to keystroke time intervals in Section 5. Section 6 reviews previous modeling efforts for latent processes with partial observability and Section 7 contains a discussion. Finally, Section 8 concludes the article. The POHMM is implemented in the `pohmm` Python package¹, and source code to reproduce the experiments in this article is available².

1. POHMM Python package: <https://github.com/vmonaco/pohmm>
2. Experiments: <https://github.com/vmonaco/pohmm-keystroke>

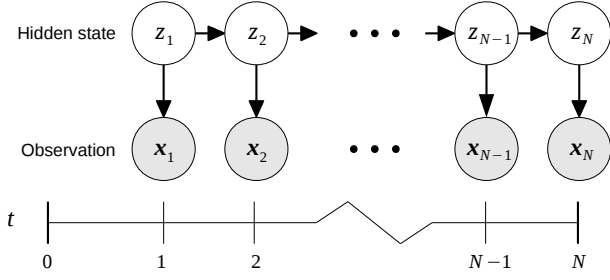


Fig. 1: Hidden Markov model [21].

2 HIDDEN MARKOV MODEL

The HMM was developed over several decades, dating back to 1960 when the forward-backward procedure was first introduced [27]. The theory was later made accessible to non-statisticians in the well-cited tutorial work, [21]. The HMM soon became popular for modeling behavioral data, such as speech, handwriting, gesture, and linguistics. More recently, it has been used to model temporal behavior, such as keystroke dynamics and terrorist activity [22], [23].

The HMM is a finite-state model in which observed values at time t depend on an underlying hidden state. The hidden state may or may not correspond to some physical state of the system, depending on the application of interest. In speech, the hidden states generally have no physical correspondence, whereas the hidden states in a model of temporal behavior might correspond to the activity levels of the system [15], [22].

The system advances in discrete steps, typically with a first-order dependency between the hidden states. At the n^{th} time step t_n , a feature vector \mathbf{x}_n is observed and the system can be in any one of M hidden states. Let \mathbf{x}_1^N be the sequence of observation vectors from time 0 to T , where N is the total number of observations. The HMM is unsupervised since it assumes the ground truth hidden state sequence is not available. The latent variable z_n is introduced to represent the hidden state at time t_n . The structure of the HMM is shown in Figure 1.

The model starts in state j at time 0 with probability π_j and transitions from state i to state j with probability a_{ij} . The transition matrix is denoted by $\mathbf{A} = [a_{ij}]$ and starting probability vector by $\pi = [\pi_j]$. The stationary probability of being in state j is given by Π_j , where

$$\Pi_j = \sum_{1 \leq i \leq M} \Pi_i a_{ij}. \quad (2)$$

The stationary probability vector Π can be computed by taking any row from the power limit of the transition matrix,

$$\lim_{n \rightarrow \infty} \mathbf{A}^n \quad (3)$$

where \mathbf{A}^n is the n^{th} matrix power. The values in column j converge to the stationary probability of state j .

While in state j at time t_n , the system emits an observation vector \mathbf{x}_n distributed according to density function $f(\cdot; \mathbf{b}_j)$ with parameter vector \mathbf{b}_j . The emission distribution can be either continuous, discrete, or a mix of both. The HMM is completely described by the number of states M ,

Algorithm 1 HMM forward algorithm.

- 1) **Initialization:** $\alpha_j(1) = f(\mathbf{x}_1; \mathbf{b}_j)\pi_j$
- 2) **Induction:** $\alpha_j(n+1) = \left(\sum_{i=1}^M \alpha_i(n)a_{ij}\right) f(\mathbf{x}_{n+1}; \mathbf{b}_j)$
- 3) **Termination:** $P(\mathbf{x}_1^N|\theta) = \sum_{j=1}^M \alpha_j(N)$

starting probabilities π , transition matrix \mathbf{A} , and emission distribution parameters \mathbf{b} . The model parameters are given by $\theta = \{\pi, \mathbf{A}, \mathbf{b}\}$.

There are generally three problems associated with the HMM [21].

- 1) Determine $P(\mathbf{x}_1^N|\theta)$, the likelihood of an observation sequence, given model parameters θ .
- 2) Determine z_1^N , the maximum likelihood sequence of hidden states, given model parameters θ and an observation sequence.
- 3) Determine $\arg \max_{\theta \in \Theta} P(\mathbf{x}_1^N|\theta)$, the maximum likelihood parameters θ , given an observation sequence.

The first and third problems are necessary for identifying and verifying users in biometric applications, while the second problem is useful for understanding user behavior. The rest of this section reviews the solutions to each of these problems and defines a two-state HMM for time intervals.

2.1 Model likelihood

Calculating $P(\mathbf{x}_1^N|\theta)$, the likelihood of an observation sequence \mathbf{x}_1^N for a given model, is necessary for user identification, in which a maximum likelihood classification is performed, and verification, in which the loglikelihood comprises a confidence score. Let the forward variable $\alpha_j(n)$ be the probability of the partial observation sequence \mathbf{x}_1^n and state j at time t_n , given model parameters θ . This can be computed inductively by Algorithm 1.

There are several ways of handling the underflow errors that will eventually occur as N increases in Algorithm 1 due to the floating point values becoming infinitesimally small. Intermediary values may be scaled or calculated in log-space. For long observation sequences, typically the loglikelihood is used. The order of computations required for the forward algorithm is $O(M^2N)$, since it requires M^2 calculations for each observation vector.

2.2 Hidden state prediction

Hidden state prediction is accomplished by the Viterbi algorithm, a dynamic programming algorithm that determines the most likely hidden state at each time step t_n . This requires estimating z_1^N , the most likely sequence of hidden states, given the observation sequence \mathbf{x}_1^N and parameters θ .

Similar to the forward variable in the previous section, the backward variable β is introduced, where $\beta_j(n)$ is the probability of the partial observation sequence \mathbf{x}_{n+1}^N and state j at time t_n , given the model parameters θ . Like the forward algorithm, the backward algorithm is $O(M^2N)$, shown in Algorithm 2.

With both the forward and backward variables, it is straightforward to calculate the posterior probability of being in state j at time t_n , given the observation sequence

Algorithm 2 HMM backward algorithm.

- 1) **Initialization:** $\beta_j(N) = 1$
- 2) **Induction:** $\beta_i(n) = \sum_{j=1}^M a_{ij} f(\mathbf{x}_{n+1}; \mathbf{b}_j) \beta_j(n+1)$
- 3) **Termination:** $P(\mathbf{x}_1^N | \theta) = \sum_{j=1}^M \beta_j(1) \pi_j$

and model parameters. This is denoted by the forward-backward variable $\gamma_j(n)$,

$$\gamma_j(n) = \frac{\alpha_j(n) \beta_j(n)}{P(\mathbf{x}_1^N | \theta)} = \frac{\alpha_j(n) \beta_j(n)}{\sum_{i=1}^M \alpha_i(n) \beta_i(n)} \quad (4)$$

where $1 \leq n \leq N$. The most likely hidden state at time t_n can then be determined by

$$z_n = \arg \max_{1 \leq j \leq M} \gamma_j(n). \quad (5)$$

2.3 Parameter estimation

Maximum likelihood (ML) parameter estimation is performed by solving $\arg \max_{\theta \in \Theta} P(\mathbf{x}_1^N | \theta)$ for parameter vector θ . This requires estimating the starting probabilities, transition probabilities, and emission distribution parameters. The starting and transition parameters have closed-form solutions, while the formula for the emission distribution parameters depends on the density function. There are closed-form solutions for multinomial, discrete binomial, Poisson, Gaussian, and Gaussian mixture distributions, among others [7].

Let $\xi_{ij}(n)$ be the probability of transitioning from state i at time t_n to state j at time t_{n+1} , given the observation sequence and model parameters θ . This can be determined using the forward and backward variables, transition probability, and emission density, given by

$$\begin{aligned} \xi_{ij}(n) &= \frac{\alpha_i(n) a_{ij} f(\mathbf{x}_{n+1}; \mathbf{b}_j) \beta_j(n+1)}{P(\mathbf{x}_1^N | \theta)} \\ &= \frac{\alpha_i(n) a_{ij} f(\mathbf{x}_{n+1}; \mathbf{b}_j) \beta_j(n+1)}{\sum_{k=1}^M \alpha_k(n) \beta_k(n)} \end{aligned} \quad (6)$$

where $1 \leq n \leq N-1$. Like the other variables, $\xi_{ij}(n)$ can be computed in $O(M^2N)$ time and stored in a $M \times M \times N-1$ matrix. Note that since $\xi_{ij}(n)$ is the probability of transitioning from state i at time t_n to state j at time t_{n+1} , the relation

$$\gamma_i(n) = \sum_{j=1}^M \xi_{ij}(n) \quad (7)$$

holds. Summing $\gamma_j(n)$ over t_n gives the expected number of transitions from state j , while summing $\xi_{ij}(n)$ over t_n gives the expected number of transitions from i to j .

The variables $\gamma_j(n)$ and $\xi_{ij}(n)$ are used to update the model parameters. The re-estimated starting probabilities are determined directly from $\gamma_j(1)$,

$$\hat{\pi}_j = \gamma_j(1). \quad (8)$$

The transition matrix is updated by the formula

$$\hat{a}_{ij} = \frac{\sum_{n=1}^{N-1} \xi_{ij}(n)}{\sum_{n=1}^{N-1} \gamma_i(n)} \quad (9)$$

Algorithm 3 HMM Baum-Welch algorithm for parameter estimation.

- 1) **Initialization**
Choose initial parameters θ^0 and let $\hat{\theta} \leftarrow \theta^0$
- 2) **Expectation**
Use $\hat{\theta}$ and \mathbf{x}_1^N to compute $\alpha_j(n)$, $\beta_j(n)$, $\gamma_j(n)$, $\xi_{ij}(n)$, and let $\hat{P} \leftarrow P(\mathbf{x}_1^N | \hat{\theta})$
- 3) **Maximization**
Update π , \mathbf{A} , and \mathbf{b} using the re-estimation formulae and let $\hat{\theta} \leftarrow \{\hat{\pi}, \hat{\mathbf{A}}, \hat{\mathbf{b}}\}$
- 4) **Termination**
If $P(\mathbf{x}_1^N | \hat{\theta}) - \hat{P} < \epsilon$ then terminate and let $\hat{\theta} \leftarrow \hat{\theta}$, otherwise go to step 2

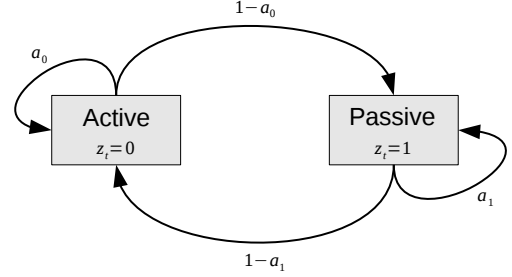


Fig. 2: Two-state hidden Markov model for temporal behavior. States correspond to activity levels of the system.

and the updated stationary probabilities are given by

$$\hat{\Pi}_j = \frac{\sum_{n=1}^N \gamma_j(n)}{\sum_{i=1}^M \sum_{n=1}^N \gamma_i(n)}. \quad (10)$$

The re-estimates for parameter vectors \mathbf{b}_j , $1 \leq j \leq M$, depend on the density function $f(\cdot)$, where

$$\hat{\mathbf{b}}_j = \arg \max_{\mathbf{b} \in \mathcal{B}} \sum_{n=1}^N \gamma_j(n) \ln f(\mathbf{x}_n; \mathbf{b}) \quad (11)$$

and \mathcal{B} is the parameter space of $f(\cdot)$. The complete parameter estimation procedure, commonly referred to as the Baum-Welch (BW) algorithm, is shown in Algorithm 3.

2.4 Hidden Markov model for time intervals

A two-state HMM of typing behavior is defined. Such a model is the simplest realization of nonhomogeneous behavior since a model with only one state leads to homogeneity. The hidden states correspond to activity levels of the user. In the active state, events are generated in quick succession, and relatively small time intervals are observed. In the passive state, relatively long time intervals are observed, and events occur less frequently. This two-state model is introduced here for the purpose of motivating and providing a benchmark against which the model proposed in Section 3 will be compared to. The resulting model is shown in Figure 2.

Human-generated time intervals generally follow a heavy-tailed distribution and are well described by a log-normal [2], [3], [4], [26]. This serves as motivation for choosing the log-normal as the density function for time intervals τ , given by

$$f(\tau; \eta, \rho) = \frac{1}{\tau \rho \sqrt{2\pi}} \exp\left(\frac{-(\ln \tau - \eta)^2}{2\rho^2}\right) \quad (12)$$

where η is the log-mean and ρ is the log-standard deviation. Note that a mixture of log-normals also gives rise to a log-normal. The log-normal parameter re-estimation formulae are given by

$$\hat{\eta}_j = \frac{\sum_{n=1}^N \gamma_j(n) \ln \tau_n}{\sum_{n=1}^N \gamma_j(n)} \quad (13)$$

and

$$\hat{\rho}_j^2 = \frac{\sum_{n=1}^N \gamma_j(n) (\ln \tau_n - \hat{\eta}_j)^2}{\sum_{n=1}^N \gamma_j(n)} \quad (14)$$

respectively. A normal distribution can be used for spatial features, where the normal density is defined as

$$f(x; \mu, \sigma) = \frac{1}{\sigma \sqrt{2\pi}} \exp\left(-\frac{(x - \mu)^2}{2\sigma^2}\right) \quad (15)$$

Parameters μ and σ are re-estimated similarly by

$$\hat{\mu}_j = \frac{\sum_{n=1}^N \gamma_j(n) x_n}{\sum_{n=1}^N \gamma_j(n)} \quad (16)$$

and

$$\hat{\sigma}_j^2 = \frac{\sum_{n=1}^N \gamma_j(n) (x_n - \hat{\mu}_j)^2}{\sum_{n=1}^N \gamma_j(n)} \quad (17)$$

where x_n is a scalar component of \mathbf{x}_n . Note that this definition assumes independence between features since covariance terms are not considered.

3 PARTIALLY OBSERVABLE HIDDEN MARKOV MODEL

In time interval data, there is often some additional information accompanying each event that gives an indication as to the hidden state. This could be the name of a key that was pressed while typing, the type of commit made to a source code repository, or some other symbol that indicates the type of action that occurred. Certain types of events may indicate a greater probability of being in a particular hidden state. For example in keystroke dynamics, the probability of being in a passive state may be greater when the Space key is pressed than any letter key since the typist is more likely to pause between words than between letters. The keyboard key name is an event type that partially reveals the hidden state. The HMM defined in the previous section fails to capture this structure since it lacks the dependence on the type of event.

Let ω be an event type that comes from a finite alphabet of size m . In the partially observable hidden Markov model, the true system state is a latent variable that depends on both the event type ω and the previous hidden state. The POHMM dependency structure is shown in Figure 3. The event types form an independent Markov chain and the hidden states depend on the event types. This structure may exist when there is a separation between the system task and system behavior. For example, typing behavior depends on the text that is typed, which could be a username and password or a response to an open-ended question. In both cases, the text is independent of typing behavior: the text is either be fixed or the result of higher cognitive processes.

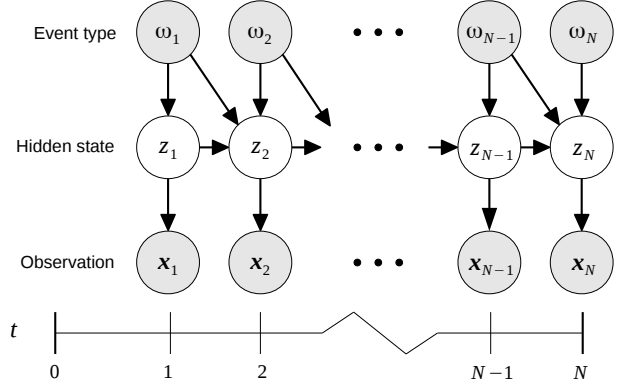


Fig. 3: Partially observable hidden Markov model structure.

TABLE 1: Summary of POHMM parameters and variables.

Parameter or Variable	Description
\mathbf{x}_1^N	Sequence of observed values, where \mathbf{x}_n may be a scalar or a vector.
Ω_1^N	Sequence of event types, where the length of Ω_1^N is N and Ω_n is the event type at time t_n .
m	The number of unique event types in Ω_1^N .
ω or ψ	Event type.
z_n	Hidden state of the system at time t_n .
M	The number of hidden states.
$a_{ij \omega, \psi}$	Probability of transitioning from state i to state j , given event types ω while in state i and ψ in state j .
$\pi_{j \omega}$	Probability of being in state j at time t_1 , given event type ω .
$\Pi_{j \omega}$	Stationary probability of being in state j , given event type ω .
$\mathbf{b}_{j \omega}$	Observation distribution parameters in state j , given event type ω .
$\gamma_{j \omega}(n)$	Posterior probability of being in state j , given observations and event type ω at time t_n .
$\xi_{ij \omega, \psi}(n)$	Posterior probability of transitioning from state i at time t_n to state j at time t_{n+1} , given event types ω and ψ at times t_n and t_{n+1} , respectively.

The HMM parameters defined in the previous section are conditioned on the event type. Specifically, model parameters include $\pi_{j|\omega}$, the probability of starting in state j , given event type ω , and $\mathbf{b}_{j|\omega}$ for the parametrized emission distribution $f(\cdot; \mathbf{b}_{j|\omega})$ that depends on event type ω . Similarly, the probability of transitioning between states i and j , given event types ω and ψ , is denoted by $a_{ij|\omega, \psi}$. A summary of POHMM parameters and variables is shown in Table 1.

Marginal distribution parameters can also be defined, in which the event type is marginalized out. Let $\pi_{j|}$ and $f(\cdot; \mathbf{b}_{j|})$ be the marginalized starting probability and emission probability, respectively. Similarly, the parameters $a_{ij|\omega, \cdot}$, $a_{ij|\cdot, \omega}$, and $a_{ij|}$ are defined as the transition probabilities after marginalizing out the second, first, and both event types, respectively. Computation of POHMM marginal distributions is covered in Section 3.5.

While the total number of parameters in the HMM is $M + M^2 + MK$, where K is the number of free parameters in the emission distribution $f(\cdot)$, the POHMM contains

Algorithm 4 POHMM forward algorithm.

- 1) **Initialization:** $\alpha_{j|\Omega_1}(1) = f(\mathbf{x}_1; \mathbf{b}_{j|\Omega_1})\pi_{j|\Omega_1}$
- 2) **Induction:**

$$\alpha_{j|\Omega_{n+1}}(n+1) = \left(\sum_{i=1}^M \alpha_{i|\Omega_n}(n) a_{ij|\Omega_n, \Omega_{n+1}} \right) f(\mathbf{x}_{n+1}; \mathbf{b}_{j|\Omega_{n+1}})$$

- 3) **Termination:** $P(\mathbf{x}_1^N | \theta, \Omega_1^N) = \sum_{j=1}^M \alpha_{j|\Omega_T}(N)$

Algorithm 5 POHMM backward algorithm.

- 1) **Initialization:** $\beta_{j|\Omega_T}(N) = 1$
- 2) **Induction:**

$$\beta_{i|\Omega_n}(n) = \sum_{j=1}^M a_{ij|\Omega_n, \Omega_{n+1}} f(\mathbf{x}_{n+1}; \mathbf{b}_{j|\Omega_{n+1}}) \beta_{j|\Omega_{n+1}}(n+1)$$

- 3) **Termination:** $P(\mathbf{x}_1^N | \theta, \Omega_1^N) = \sum_{j=1}^M \beta_{j|\omega}(1) \pi_{j|\omega}$

$m \times (M + mM^2 + MK)$ parameters³. After accounting for normalization constraints, the number of degrees of freedom (*dof*) is $m \times (M - 1 + mM(M - 1) + MK)$, corresponding to the number of free parameters. This will reduce further after parameter smoothing strategies are applied, as discussed in Section 3.6.

3.1 Model likelihood

The POHMM likelihood is computed by a modified forward procedure, similar to the HMM. At each time step t_n , the system emits an event with type Ω_n and is in 1 out of M hidden states. The model likelihood is given by $P(\mathbf{x}_1^N | \theta, \Omega_1^N)$, which is the probability of the observation sequence, given both the model parameters θ and the sequence of event types Ω_1^N . This can be calculated using the conditional model parameters $\pi_{j|\omega}$, $a_{ij|\omega, \psi}$, and $\mathbf{b}_{j|\omega}$ for hidden states $1 \leq j \leq M$ and event types $\omega, \psi \in \Omega_1^N$. The modified forward algorithm and backward algorithm for the POHMM are shown in Algorithms 4 and 5, respectively.

The model likelihood may be obtained by either algorithm upon termination. Note that like the HMM, the modified forward and backward algorithms both take $O(M^2N)$ time to compute. The forward variable $\alpha_{j|\Omega_n}(n)$ is the probability of observing the sequence \mathbf{x}_1^n and being in state j at time t_n , given the model parameters θ and the event type sequence Ω_1^n with event type Ω_n at time t_n . Similarly, the backward variable $\beta_{j|\Omega_n}(n)$ is the probability of the observing the sequence \mathbf{x}_n^N and being in state j at time t_n , given model parameters θ and event type sequence Ω_n^N with event type Ω_n at time t_n .

3.2 Hidden state prediction

Determination of the most likely sequence of hidden states proceeds similar to the HMM, using the event type-dependent parameters. First, the posterior probability of

being in state j at time t_n , given event type Ω_n , is defined using the POHMM forward and backward variables

$$\begin{aligned} \gamma_{j|\Omega_n}(n) &= \frac{\alpha_{j|\Omega_n}(n) \beta_{j|\Omega_n}(n)}{P(\mathbf{x}_1^N | \theta, \Omega_1^N)} \\ &= \frac{\alpha_{j|\Omega_n}(n) \beta_{j|\Omega_n}(n)}{\sum_{i=1}^M \alpha_{i|\Omega_n}(n) \beta_{i|\Omega_n}(n)}. \end{aligned} \quad (18)$$

Hidden states are then taken as the maximum likelihood states at each time step,

$$z_n = \arg \max_{1 \leq j \leq M} \gamma_{j|\Omega_n}(n). \quad (19)$$

3.3 Parameter estimation

Parameter estimation is similar to the HMM, where the POHMM uses a modified Baum-Welch algorithm. Using the modified forward-backward variable given by Equation 18, the POHMM starting probabilities are

$$\hat{\pi}_{j|\omega} = \gamma_{j|\Omega_1}(1) \quad (20)$$

where $\omega = \Omega_1$.

Generally, it may not be possible to estimate $\hat{\pi}_{j|\omega}$ for many ω due to there only being one Ω_1 (or several Ω_1 for multiple observation sequences). To deal with this, parameter smoothing is introduced in Section 3.6.

To complete the equations for updating parameters in the modified Baum-Welch algorithm, the POHMM analogue of $\xi_{ij}(t)$ defined for the HMM in Equation 6 is needed. Let $\xi_{ij|\Omega_n, \Omega_{n+1}}(n)$ be the probability of transitioning from state i at time t_n to state j at time t_{n+1} , given event types Ω_n at time t_n and Ω_{n+1} at time t_{n+1} as well as the observation sequence and model parameters θ . Using the POHMM forward and backward variables, this is given by

$$\begin{aligned} \xi_{ij|\Omega_n, \Omega_{n+1}}(n) &= \frac{\alpha_{i|\Omega_n}(n) a_{ij|\Omega_n, \Omega_{n+1}} f(\mathbf{x}_{n+1}; \mathbf{b}_{j|\Omega_{n+1}}) \beta_{j|\Omega_{n+1}}(n+1)}{P(\mathbf{x}_1^N | \theta, \Omega_1^N)}, \\ & \quad 1 \leq n \leq N-1. \end{aligned} \quad (21)$$

Note that computing $\xi_{ij|\omega, \psi}(n)$ for the POHMM can be performed time linear in the number of observations, $O(M^2N)$, since the event types are not enumerated at each time step.

Next, the transition probabilities are estimated. In contrast to the HMM, which has M^2 transition probabilities, there are m^2M^2 transition probabilities in the POHMM. Computing the updated transition probabilities can be performed in $O(M^2N)$ time. The equation is

$$\begin{aligned} \hat{a}_{ij|\omega, \psi} &= \frac{\sum_{n \in \mathcal{T}_{\omega, \psi}} \xi_{ij|\Omega_n, \Omega_{n+1}}(n)}{\sum_{n \in \mathcal{T}_{\omega, \psi}} \gamma_{i|\Omega_n}(n)}, \\ \mathcal{T}_{\omega, \psi} &= \{n | \Omega_n = \omega, \Omega_{n+1} = \psi\} \end{aligned} \quad (22)$$

where $\mathcal{T}_{\omega, \psi} = \{n | \Omega_n = \omega, \Omega_{n+1} = \psi\}$ is the set of indexes at which event type ω is observed at time t_n and ψ is observed at time t_{n+1} . Note that $\hat{a}_{ij|\omega, \psi}$ requires only the transitions between event types ω and ψ .

3. This does not include marginal distribution parameters.

Algorithm 6 POHMM modified Baum-Welch algorithm.

- 1) **Initialization**
Choose initial parameters θ^0 and let $\hat{\theta} \leftarrow \theta^0$
- 2) **Expectation**
Use $\hat{\theta}$, \mathbf{x}_1^N , Ω_1^N to compute $\alpha_{j|\Omega_n}(n)$, $\beta_{j|\Omega_n}(t)$, $\gamma_{j|\Omega_n}(n)$, $\xi_{ij|\Omega_n, \Omega_{n+1}}(n)$, let $\dot{P} \leftarrow P(\mathbf{x}_1^N | \hat{\theta}, \Omega_1^N)$
- 3) **Maximization**
Update π , \mathbf{A} , and \mathbf{b} using the re-estimation formulae and let $\hat{\theta} \leftarrow \{\hat{\pi}, \hat{\mathbf{A}}, \hat{\mathbf{b}}\}$
- 4) **Termination**
If $P(\mathbf{x}_1^N | \hat{\theta}, \Omega_1^N) - \dot{P} < \epsilon$ then terminate and let $\hat{\theta} \leftarrow \hat{\theta}$, otherwise go to step 2

Estimating the emission distribution parameters depends on the density function $f(\cdot)$, where the new estimates are given by

$$\hat{\mathbf{b}}_{j|\omega} = \arg \max_{\mathbf{b} \in \mathcal{B}} \sum_{n \in \mathcal{T}_\omega} \gamma_{j|\Omega_n}(n) \ln f(\mathbf{x}_n; \mathbf{b}),$$

$$\mathcal{T}_\omega = \{n | \Omega_n = \omega\} \quad (23)$$

As an example, the normal emission distribution parameters are estimated for the POHMM, conditioned on the event type. Using the forward-backward variable from Equation 18,

$$\hat{\mu}_{j|\omega} = \frac{\sum_{n \in \mathcal{T}_\omega} \gamma_{j|\Omega_n}(n) \mathbf{x}_n}{\sum_{n \in \mathcal{T}_\omega} \gamma_{j|\Omega_n}(n)},$$

$$\mathcal{T}_\omega = \{n | \Omega_n = \omega\} \quad (24)$$

and

$$\hat{\sigma}_{j|\omega}^2 = \frac{\sum_{n \in \mathcal{T}_\omega} \gamma_{j|\Omega_n}(n) (\mathbf{x}_n - \hat{\mu}_{j|\omega})^2}{\sum_{n \in \mathcal{T}_\omega} \gamma_{j|\Omega_n}(n)},$$

$$\mathcal{T}_\omega = \{n | \Omega_n = \omega\} \quad (25)$$

are the updated mean and variance estimates for hidden state j , given event type ω . Note that the estimates depend only on the elements of $\gamma_{\Omega_n}(n)$ where $\Omega_n = \omega$. The log-normal POHMM emission parameters are re-estimated similarly.

The modified Baum-Welch algorithm, which uses Equations 20, 22, and 23 to update model parameters in each iteration, is shown in Algorithm 6. The convergence criterion is a threshold ϵ on the loglikelihood reduction. The rest of this section deals with other aspects of parameter estimation, including initialization, marginal distributions, and parameter smoothing.

3.4 Parameter initialization

Parameter initialization is an important step in the Baum-Welch algorithm and may ultimately determine the quality of the estimated parameters. Initial parameters may either be chosen randomly or derived from the observations. This work uses an observation-based parameter initialization procedure that guarantees reproducible parameter estimates.

The starting and transition probabilities are simply initialized as

$$\pi_{j|\omega} = \frac{1}{M} \quad (26)$$

and

$$a_{ij|\omega, \psi} = \frac{1}{M} \quad (27)$$

for all i, j, ω , and ψ . This reflects a maximum entropy distribution (i.e., uniform distribution) in the absence of any starting or transition priors.

Next, the emission density parameters are initialized. The strategy proposed here is to initialize parameters in such a way that there is a correspondence between hidden states from two different models. That is, for any two models, hidden state $j = 1$ corresponds to the active state and $j = 2$ corresponds to the passive state. Using a log-normal emission distribution, this is accomplished by spreading the log-mean initial parameters. Let

$$\eta_\omega = \frac{\sum_{n \in \mathcal{T}_\omega} \ln \mathbf{x}_n}{|\mathcal{T}_\omega|}, \quad \mathcal{T}_\omega = \{n | \Omega_n = \omega\} \quad (28)$$

and

$$\rho_\omega^2 = \frac{\sum_{n \in \mathcal{T}_\omega} (\ln \mathbf{x}_n - \eta_{j|\omega})^2}{|\mathcal{T}_\omega|}, \quad \mathcal{T}_\omega = \{n | \Omega_n = \omega\} \quad (29)$$

be the log-mean and log-variance of observations in \mathbf{x}_1^N , conditioned on event type ω . The model parameters are then initialized as

$$\eta_{j|\omega} = \eta_\omega + \left(\frac{2h(j-1)}{M-1} - h \right) \times \rho_\omega \quad (30)$$

and

$$\rho_{j|\omega}^2 = \rho_\omega^2 \quad (31)$$

for $1 \leq j \leq M$, where h is a bandwidth parameter that determines the spread. In a two-state model, this ensures that state $j = 1$ corresponds to the state with the smaller log-mean time interval.

3.5 Marginal distributions

When computing the likelihood of a novel sequence, it is possible that some event types in the novel sequence were not observed during parameter estimation. For example, this situation can occur when event types correspond to key names of freely-typed text and novel keys are observed during testing. A fallback mechanism (sometimes referred to as a "backoff" model) is typically employed to handle missing data during training and novel data during testing, such as those used in keystroke [18], [28] and linguistics [12]. In order for the POHMM to handle missing or novel event types during likelihood calculation, the marginal distributions are used. This creates a two-level fallback hierarchy in which missing or novel event types fall back to the distribution in which the event type is marginalized out.

Let the probability of event type ω at time t_1 be π_ω , and the probability of transitioning from event type ω to ψ be denoted by $a_{\omega, \psi}$. Both of these can be computed directly from the event type sequence Ω_1^N . The marginal probability $\pi_{j|}$ is the probability of starting in hidden state j , in which the event type has been marginalized out, given by

$$\pi_{j|} = \sum_{\omega \in \Omega} \pi_{j|\omega} \pi_\omega \quad (32)$$

where Ω is the set of unique event types in Ω_1^N .

Marginal transition probabilities can also be calculated. Let $a_{ij|\omega}$ be the probability of transitioning from hidden state i to hidden state j , given event type ω while in hidden state i . The second event type for hidden state j has been marginalized out. This probability is given by

$$a_{ij|\omega} = \sum_{\psi \in \Omega} a_{ij|\omega, \psi} a_{\omega, \psi} \quad (33)$$

The marginal probability $a_{ij|\cdot}$ is defined similarly by

$$a_{ij|\cdot} = \frac{\sum_{\omega \in \Omega} a_{ij|\omega, \psi} a_{\omega, \psi}}{\sum_{\omega \in \Omega} a_{\omega, \psi}} \quad (34)$$

Finally, the marginal $a_{ij|\cdot}$ is the probability of transitioning from hidden state i to j ,

$$a_{ij|\cdot} = \frac{1}{m} \sum_{\omega \in \Omega} \sum_{\psi \in \Omega} a_{ij|\omega, \psi} a_{\omega, \psi} \quad (35)$$

No denominator is needed in Equation 33 since the normalization constraints of both transition matrices carry over to the left-hand side. Equation 35 is normalized by $\frac{1}{m}$ since $\sum_{\omega \in \Omega} \sum_{\psi \in \Omega} a_{\omega, \psi} = m$ where m is the number of unique event types in Ω .

The marginal emission distribution is a mixture of the emission distributions conditioned on each of the event types. For normal and log-normal emissions, the marginal emission is simply a mixture of normals or log-normals, respectively. Let $\mu_{j|\cdot}$ and $\sigma_{j|\cdot}^2$ be the mean and variance of the marginal distribution for hidden state j . The marginal mean is a weighted sum of the conditional distributions, given by

$$\mu_{j|\cdot} = \sum_{\omega \in \Omega} \Pi_{\omega} \mu_{j|\omega} \quad (36)$$

where Π_{ω} is the stationary probability of event type ω . This can be calculated directly from the event type sequence Ω_1^T , where

$$\Pi_{\omega} = \frac{1}{N} \sum_{n=1}^N I(\Omega_n = \omega) \quad (37)$$

and $I(\cdot)$ is the indicator function. Similarly, the marginal variance is given by

$$\sigma_{j|\cdot}^2 = \sum_{\omega \in \Omega} \Pi_{\omega} \left[(\mu_{j|\omega} - \mu_{j|\cdot})^2 + \sigma_{j|\omega}^2 \right]. \quad (38)$$

Calculation of the marginalized log-normal distribution parameters is exactly the same.

3.6 Parameter smoothing

While the marginal distributions can be used to handle missing or novel data during likelihood calculation, parameter smoothing handles missing or infrequent data during parameter estimation. The purpose of parameter smoothing is twofold. First, it reduces the *dof* of the model to avoid overfitting, a problem often encountered when there is a large number of parameters and small number of observations. Second, parameter smoothing provides superior estimates in the case of missing or infrequent data. For motivation, consider a keystroke letter sequence of length N . There are at most 27 unique keys that can be observed,

Algorithm 7 POHMM parameter estimation.

- 1) **Initialization**
Choose initial parameters θ^0 and let $\hat{\theta} \leftarrow \theta^0$
- 2) **Expectation**
Use $\hat{\theta}$, \mathbf{x}_1^N , Ω_1^N to compute $\alpha_{j|\Omega_n}(n)$, $\beta_{j|\Omega_n}(n)$, $\gamma_{j|\Omega_n}(n)$, $\xi_{ij|\Omega_n, \Omega_{n+1}}(n)$, let $\dot{P} \leftarrow P(\mathbf{x}_1^N | \hat{\theta}, \Omega_1^N)$
- 3) **Maximization**
Update π , \mathbf{A} , and \mathbf{b} using the re-estimation formulae and let $\hat{\theta} \leftarrow \{\hat{\pi}, \hat{\mathbf{A}}, \hat{\mathbf{b}}\}$
- 4) **Marginal distributions**
Calculate marginal distributions
- 5) **Parameter smoothing**
Calculate smoothing weights and smooth the parameters with marginals
- 6) **Termination**
If $P(\mathbf{x}_1^N | \hat{\theta}, \Omega_1^N) - \dot{P} < \epsilon$ then terminate and let $\hat{\theta} \leftarrow \hat{\theta}$, otherwise go to step 2

including the Space key, and 27×27 unique digrams (subsequences of length 2). Most of these will rarely, or never, be observed in a typing sample of English text. Additionally, it is possible that some sequences encountered in the testing phase were not observed during parameter estimation. The POHMM handles this sparsity by mixing the conditional and marginal distributions for each set of parameters.

After parameter smoothing, each parameter in the POHMM becomes a weighted average with the corresponding marginal parameters. An inverse frequency weighting strategy uses the event type frequencies to define the weights as

$$w_{\omega} = 1 - \frac{1}{1 + f(\omega)} \quad (39)$$

where $f(\omega) = \sum_{t=1}^N I(\Omega_t = \omega)$ is the frequency of event type ω in the sequence Ω_1^N . This ensures that parameters remain asymptotically unbiased as $N \rightarrow \infty$. For finite N , parameters dependent on infrequent event types will be more heavily biased towards the marginal distribution, while parameters dependent on frequently occurring event types will be largely unbiased. Other weighting strategies are possible, such as using the stationary event type probabilities, Π_{ω} , or fixed weights. While this work uses the inverse frequency weighting strategy defined above, the choice of optimal weights remains an open question and could, perhaps, reflect some prior on the observation sequence.

The POHMM starting probabilities are smoothed by

$$\pi_{j|\omega} = w_{\omega} \pi_{j|\omega} + (1 - w_{\omega}) \pi_{j|\cdot}$$

for each $\omega \in \Omega$. This ensures that the starting probability conditioned on infrequent or missing event types is estimated using some knowledge from the marginalized starting probability. Similarly, emission parameters are smoothed by

$$\mathbf{b}_{j|\omega} = w_{\omega} \mathbf{b}_{j|\omega} + (1 - w_{\omega}) \mathbf{b}_{j|\cdot}$$

The smoothing weights for transition probabilities follow similar formulae. Let $f(\omega, \psi)$ be the frequency of event type ω followed by ψ in the sequence Ω_1^T . Weights for the

conditional and marginal transition probabilities are defined as

$$\begin{aligned} w_{\omega} &= \frac{1}{f(\omega, \psi) + f(\psi)} \\ w_{\psi} &= \frac{1}{f(\omega, \psi) + f(\omega)} \\ w_{\omega, \psi} &= 1 - \left(\frac{1}{f(\omega, \psi) + f(\omega)} + \frac{1}{f(\omega, \psi) + f(\psi)} \right) \\ w_{..} &= 0 \end{aligned} \quad (40)$$

where $w_{\omega, \psi} + w_{\omega} + w_{\psi} + w_{..} = 1$. The smoothed parameter transition matrix is given by

$$a_{ij|\omega, \psi} = w_{\omega, \psi} a_{ij|\omega, \psi} + w_{\omega} a_{ij|\omega} + w_{\psi} a_{ij|\psi} + w_{..} a_{ij|..} \quad (41)$$

In this strategy, the weight for the marginal $a_{ij|..}$ is 0, although in other strategies this could be non-zero. The POHMM parameter estimation procedure, including marginal calculations and parameter smoothing, is given by Algorithm 7.

4 SIMULATION STUDY

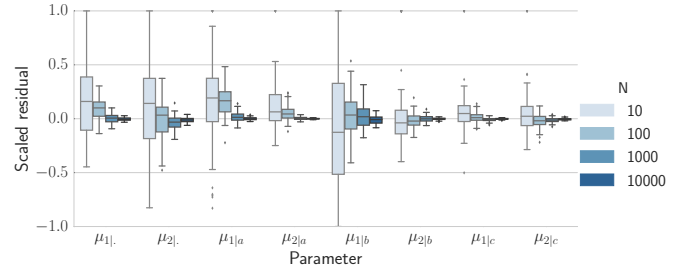
It is important for statistical models to be consistent [19]. This requires that parameter estimation be both convergent and asymptotically unbiased. While the BW algorithm for HMM parameter estimation has these properties, it is not clear whether the modified BW for POHMM parameter estimation also does. Specifically, parameter smoothing may violate the maximization step in the EM algorithm.

Consistency of the POHMM implementation is demonstrated in this section using computational methods. First, a model is initialized with parameters θ_0 . From this model, S samples are generated, each containing N time intervals. For each set of samples, the best-estimate parameters $\hat{\theta}$ are computed using the modified BW algorithm in Algorithm 7. As N increases, with sufficiently large S , the scaled residuals of a consistent model will go to 0. Convergence to 0 should also be insensitive to the choice of θ_0 . Let $\hat{\theta}_N$ be the parameters determined by the modified BW algorithm for an observed time series of length N generated from a POHMM with true parameters θ^0 . The model is consistent if

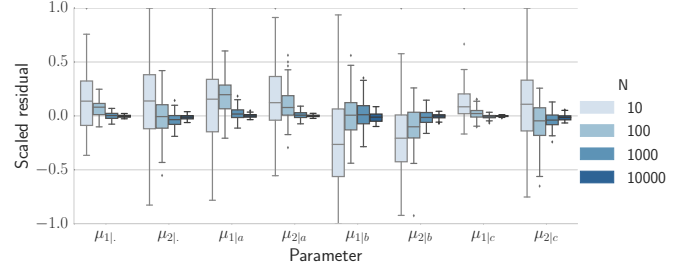
$$\lim_{N \rightarrow \infty} \frac{|\hat{\theta}_N - \theta^0|}{\max_{\hat{\theta}} |\hat{\theta}_N - \theta^0|} = \mathbf{0}. \quad (42)$$

This procedure requires generating a random POHMM in which certain parameter constraints must be met. The event type starting and transition probabilities are first generated, followed by the conditional hidden state transition matrices. Marginal distributions are determined as described in Section 3.5. Rows of the transition matrices are uniformly distributed and must sum to 1.

A POHMM with 3 event types, $\Omega = \{a, b, c\}$, and 2 hidden states is generated. A normal distribution is chosen for the emission, with mean and standard deviation comparable to human key-press time intervals. For each value of N , 100 length- N samples are generated. Each sample consists of the observation sequence and event type sequence. To generate a sample, first N event types are generated according to the event type transition matrix, which forms a Markov chain.

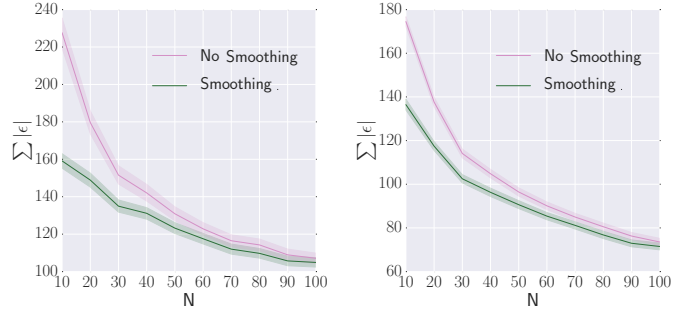


(a) μ scaled residuals without smoothing



(b) μ scaled residuals with smoothing

Fig. 4: Scaled residuals for μ conditioned on each event type without (top) and with (bottom) inverse frequency parameter smoothing. Central lines indicate the median, boxes depict the interquartile range, and whiskers show the 95% confidence interval. Outliers are shown as points outside the whiskers.



(a) μ parameters

(b) σ parameters

Fig. 5: Parameter estimation residuals without and with parameter smoothing as N increases. The sum of absolute residuals is calculated for all μ and σ parameters (excluding the marginals). Smoothing generally results in better estimates as demonstrated by the smaller residuals. Bands show the 95% confidence intervals.

The hidden states and emissions are then generated based on the event type sequence.

Figure 4a shows the scaled residuals of the marginal and conditional μ parameters without parameter smoothing. The residuals tend toward 0 as N increases, indicating convergent and unbiased estimates. The same test is repeated with a POHMM that uses parameter smoothing

TABLE 2: Keystroke data summary. Columns indicate: number of users, samples per user, keystrokes per Sample, and $\bar{\tau}$ =mean press-press latency (milliseconds).

Dataset	Ref.	Users	Samples	Keyst.	$\bar{\tau}$
Password	[13]	51	400	11	249
Keypad	[1]	30	20	11	376
Mobile	[11]	51	20	11	366
Fixed-text	[18]	60	4	100	264
Free-text	[30]	55	6	500	284

as described in Section 3.6. The scaled residuals are shown in Figure 4b. The results indicate the model is consistent, as the scaled residuals of the smoothed model tend toward 0. Model consistency with parameter smoothing can also be demonstrated analytically. As N increases, the frequency of each event type increases and the effect of parameter smoothing is diminished. Smoothing weights of the marginal parameters approach 0 in limit, and weights for the conditional parameters approach 1. Figure 5 shows the sum of absolute residuals for all μ and σ parameters (excluding marginals), comparing the smoothed parameter residuals to those obtained without smoothing. Parameter smoothing provides superior estimates, especially with a small number of observations.

5 APPLICATION TO KEYSTROKE BIOMETRICS

Five publicly-available keystroke datasets are analyzed in this section, summarized in Table 2. The *password*, *keypad*, and *mobile* datasets contain short fixed-text input in which all the users in each dataset typed the same 10-character string followed by the Enter key: “.tie5Roanl” for the password dataset [13] and “9141937761” for the keypad and mobile datasets [1], [11]. Samples that contained errors or more than 11 keystrokes were discarded. The password dataset was collected on a laptop keyboard equipped with a high-resolution clock, while timestamps in all other datasets have millisecond resolution⁴. The keypad dataset used a 10-digit numeric keypad [1], located on the right side of many standard desktop keyboards, and the mobile dataset used a soft keypad with similar layout [11]. The mobile dataset includes additional sensors measured on each key press and release event, including accelerometer, gyroscope, screen location, and pressure.

The *fixed-text* dataset contains long fixed-text input from 60 users who each copied 4 different nursery rhymes or fables [18], [30]. Since mistakes were permitted, the keystrokes for the same copy task varied, unlike the short fixed-text datasets above. The *free-text* dataset contains long free-text input from 55 users who each answered 6 essay-style questions as part of a class exercise [30]. Both the fixed-text and free-text datasets were collected on standard desktop and laptop keyboards. For this work, the fixed-text samples were truncated to each contain exactly 100 keystrokes and the free-text samples to each contain exactly 500 keystrokes.

The two-state POHMM defined in Section 3 assumes that the user can be in either an active or passive state of

4. Clock resolution is the degree to which a measurement can be made and clock precision is the degree to which a measurement can be repeated.

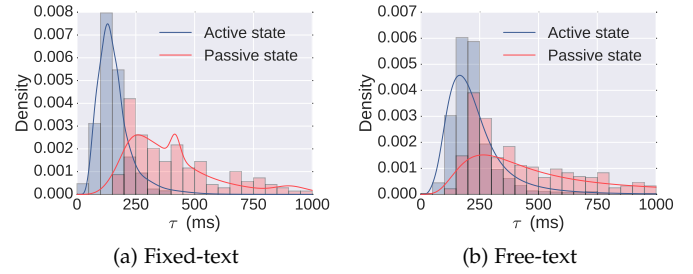


Fig. 6: POHMM marginal time interval distributions showing a separation between active and passive typing states. The distribution of each hidden state is a mixture of log-normals for each event type.

typing, and the keyboard key names are event types that partially reveal the hidden state. Each keystroke event emits two timing features

$$\tau_n = t_n^P - t_{n-1}^P \quad (43)$$

$$d_n = t_n^R - t_n^P \quad (44)$$

where t_n^P and t_n^R are the press and release timestamps of the n^{th} keystroke, respectively. The press-press time interval, τ , and key-hold duration, d , are each modeled by a log-normal distribution conditioned on the hidden state and key name. The POHMM parameters are determined using Algorithm 7, and convergence is achieved after a loglikelihood reduction of 10^{-6} , or 1000 iterations, whichever is reached first. As an example, the POHMM marginal time interval distributions for each hidden state are shown in Figure 6 for two randomly-select keystroke samples. The passive state in the free-text model has a heavier tail than the fixed-text, while the active state distributions in both models are comparable. The rest of this section presents experimental results for a goodness of fit test, identification, verification, and continuous verification.

5.1 Goodness of fit

To determine whether the proposed model is consistent with observed data, a Monte Carlo goodness of fit test is performed. The test proceeds as follows. For each keystroke sample (using the key-press time intervals only), the model parameters $\hat{\theta}_m$ are determined. The area test statistic between the model and empirical distribution is then taken. The area test statistic is a compromise between the Kolmogorov-Smirnov (KS) test and Cramér-von Mises test [16], given by

$$A = \int |P_D(\tau) - P_M(\tau|\hat{\theta}_m)| d\tau \quad (45)$$

where P_D is the empirical cumulative distribution and P_M is the model cumulative distribution.

The marginal density of the POHMM is given by

$$g(\mathbf{x}; \theta) = \sum_{\omega \in \Omega} \sum_{j=1}^M \Pi_{\omega} \Pi_j f(\mathbf{x}; \mathbf{b}_j | \omega) \quad (46)$$

where Π_j is the stationary probability of hidden state j and Π_{ω} is the stationary probability of event type ω . Using the

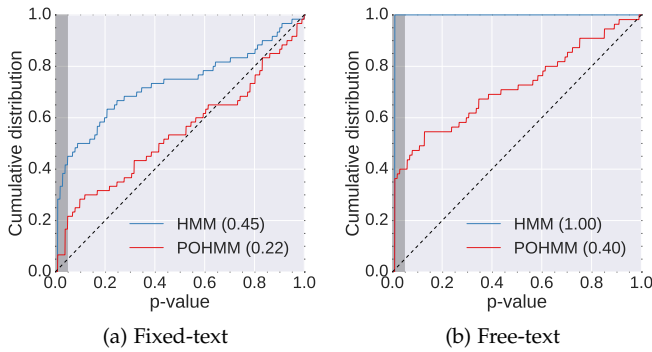


Fig. 7: Keystroke goodness of fit p-value distributions testing the null hypothesis that the model is consistent with the data. Proportions of rejected samples at the 0.05 significance level are shown in parentheses. If the null hypothesis was true, i.e., the model was actually consistent with the keystroke data, then p-values would follow a uniform distribution shown by the dashed black line.

fitted model with parameters $\hat{\theta}_m$, a surrogate data sample the same size as the empirical data is then generated. The surrogate data is treated similarly to the empirical data, and estimated parameters $\hat{\theta}_s$ are determined using the surrogate observations. The area test statistic between the surrogate-data-trained model and surrogate data is computed, given by A_s . This process repeats until enough surrogate statistics have accumulated to reliably determine $P(|A_s - \langle A_s \rangle| > |A - \langle A_s \rangle|)$. The biased p-value is given by

$$\frac{I(|A_s - \langle A_s \rangle| > |A_m - \langle A_s \rangle|) + 1}{m + 1} \quad (47)$$

where $I(\cdot)$ is the indicator function. The null hypothesis, that the model is consistent with the data, is tested for each sample in each dataset. Each test requires fitting $S + 1$ models (1 empirical and S surrogate samples).

The test is performed for both the HMM and the POHMM for each user in the fixed-text and free-text datasets, using the key-press time intervals only. The resulting p-value distributions are shown in Figure 7. The shaded area represents a 0.05 significance level in which the null hypothesis is rejected. For the fixed-text dataset, the HMM is rejected for 45% of users, while the POHMM is rejected for 22% of users. The HMM is rejected for 100% of users in the free-text dataset, and the POHMM is rejected for 40% of users. If the POHMM truly reflected typing behavior (i.e., the null hypothesis was actually true), the p-values would follow a uniform distribution shown by the dashed black line.

5.2 Identification and verification

As a statistical model, the POHMM can perform anomaly detection and can be used for biometric identification and verification. Given a query sample from an unknown user, identification is performed by choosing the user model with maximum likelihood from a population of models. Verification is performed by comparing the normalized likelihood of a query sample under a particular user model to a threshold.

Identification and verification results are obtained for each keystroke dataset and four benchmark anomaly detectors in addition to the POHMM. The password dataset uses a validation procedure similar to [13], except only samples from the 4th session (repetitions 150-200) are used for training and sessions 5-8 (repetitions 201-400) for both genuine and impostor users are used for testing. For the other datasets, results are obtained through a stratified cross-fold validation procedure with the number of folds equal to the number of samples per user: 20 for keypad and mobile, 4 for fixed-text, and 6 for free-text. In each fold, one sample from each user is retained as a query and the remaining samples are used to train a model for each user.

Identification accuracy (ACC) is measured by the proportion of correctly classified query samples. Verification performance is measured by the user-dependent equal error rate (EER), the point on the receiver operating characteristic (ROC) curve at which the probabilities of false acceptance and false rejection are equal. Each query sample is compared against every model in the population, only one of which will be genuine. The resulting loglikelihood is normalized using the minimum and maximum loglikelihoods from every model in the population to obtain a normalized score between 0 and 1. Confidence intervals for both the ACC and user-dependent EER are obtained over users in each dataset, similar to [13].

Benchmark anomaly detectors include Manhattan distance, scaled Manhattan distance, one-class support vector machine (SVM), and a standard two-state HMM. The Manhattan, scaled Manhattan, and one-class SVM operate on fixed-length feature vectors, unlike the HMM and POHMM. Timing feature vectors for the password, keypad, and mobile datasets are formed by the 11 press-press latencies and 10 durations of each 11-keystroke sample for a total of 21 timing features. The mobile sensors provide an additional 10 features for each keystroke event for a total of 131 features. For each event, the sensor features include: acceleration (meters/second²) and rotation (radians/second) along three orthogonal axes (6 features), screen coordinates (2 features), pressure (1 feature), and the length of the major axis of the ellipse fit to the pointing device (1 feature). Feature vectors for the fixed-text and free-text datasets are each comprised of a set of 218 descriptive statistics for various keystroke timings. Such timing features include the sample mean and standard deviation duration of various sets of keys, e.g., consonants, and latency between sets of keys, e.g., from consonants to vowels. For a complete list of features see [18], [29]. The free and fixed-text feature extraction also includes a rigorous outlier removal step which excludes observations that fall outside a specified confidence interval. A hierarchical fallback scheme accounts for missing or infrequent observations.

The Manhattan anomaly detector uses the negative Manhattan distance to the mean template vector as a confidence score, as described in [13]. For the scaled Manhattan detector, features are first scaled by the inverse of the global mean absolute deviation. This differs slightly from the scaled Manhattan in [13], which uses the mean absolute deviation of each template. The global mean absolute deviation is used in this work due to the low number of samples per user for some datasets. The one-class SVM uses a radial basis

TABLE 3: Identification accuracy. Bold indicates systems that are not significantly worse than the best system.

	Manhattan	Manhattan (scaled)	SVM (one-class)	HMM	POHMM
Password	0.510 (0.307)	0.662 (0.282)	0.465 (0.293)	0.467 (0.295)	0.789 (0.209)
Keypad	0.623 (0.256)	0.713 (0.200)	0.500 (0.293)	0.478 (0.287)	0.748 (0.151)
Mobile (w/o sensors)	0.290 (0.230)	0.528 (0.237)	0.267 (0.229)	0.303 (0.265)	0.607 (0.189)
Mobile (w/ sensors)	0.647 (0.250)	0.947 (0.104)	0.857 (0.232)	0.937 (0.085)	0.971 (0.039)
Fixed-text	0.492 (0.332)	0.613 (0.314)	0.571 (0.235)	0.392 (0.355)	0.887 (0.175)
Free-text	0.730 (0.320)	0.839 (0.242)	0.342 (0.302)	0.303 (0.351)	0.909 (0.128)

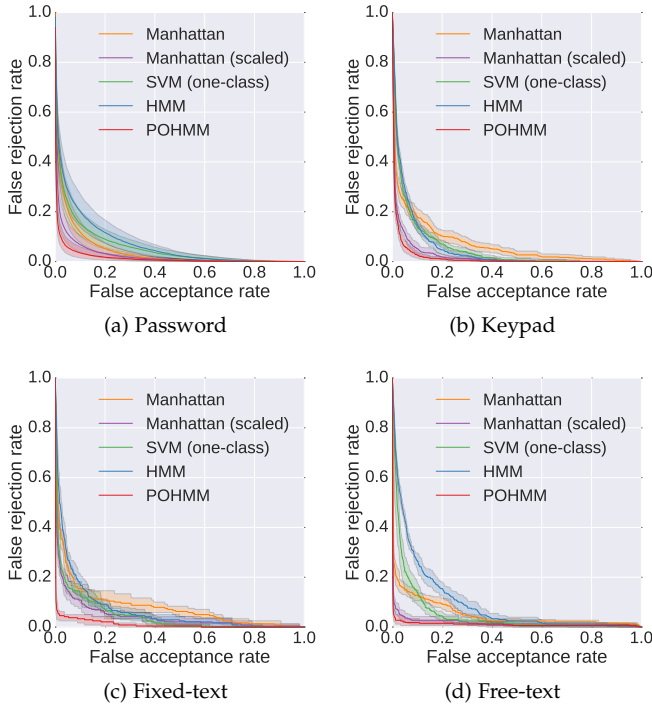


Fig. 8: Keystroke ROC curves. Bands show the 95% confidence intervals.

function (RBF) kernel and 0.5 tolerance of training errors, i.e., half the samples will become support vectors. The HMM is the model defined in Section 2, which has two hidden states and key-press time interval and duration emissions each modeled by a log-normal distribution. The POHMM is exactly the same as the HMM, except the hidden states are conditioned on the key names.

Identification and verification results are shown in Tables 3 and 4, respectively, and ROC curves for the password, keypad, fixed-text, and free-text datasets are shown in Figure 8. The best-performing anomaly detectors in Tables 3 and 4 are shown in bold. The set of best-performing detectors contains those that are not significantly worse than the POHMM, which achieves the highest performance in every experiment. The Wilcoxon signed-rank test is used to determine whether a detector is significantly worse than the best detector, testing the null hypothesis that a detector has the same performance distribution as the POHMM. A Bonferroni correction is applied to control the familywise error rate, which is the probability of falsely rejecting a

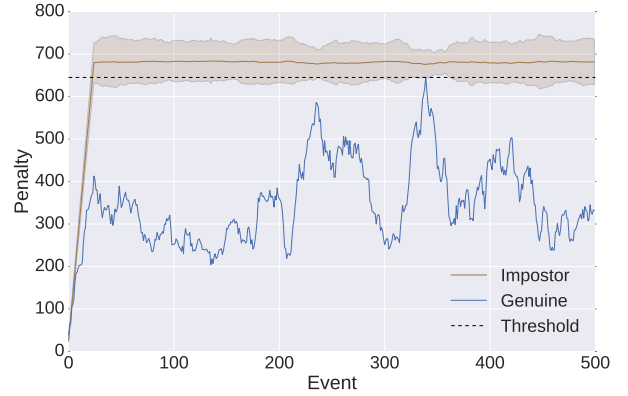


Fig. 9: Continuous verification example. Bands show the 95% confidence interval. In this example, impostors are detected after an average of 81 keystrokes.

detector that is actually in the set of best-performing detectors [24]. At a 0.05 significance level, the null hypothesis is rejected with a p-value not greater than $\frac{0.05}{4}$, since four tests are applied in each row. The POHMM achieves the highest identification accuracy and lowest equal error rate for each dataset. For 3 out of 6 datasets in both sets of experiments (identification and verification), all other detectors are found to be significantly worse than the POHMM.

5.3 Continuous verification

Keystrokes are continuously generated as the user interacts with a computer system. In an intrusion detection scenario, it is desirable to detect an impostor within as few keystrokes as possible. This differs from the static verification scenario in the previous section in which keystrokes were partitioned into sessions and a verification decision was made for each session. Instead, continuous verification requires a verification decision to be made upon each new keystroke [6].

Continuous verification is enforced through a penalty function in which each new keystroke incurs a non-negative penalty. The penalty at any given time can be thought of as the inverse of trust. As behavior becomes more consistent with the model, the cumulative penalty within the window can decrease, and as it becomes more dissimilar, the penalty increases. The user is rejected from the system, i.e., labeled as an impostor, if the cumulative penalty within a sliding window exceeds a threshold. The threshold is determined for each sample such that the genuine user is never labeled as an impostor, analogous to a 0% false rejection rate in static verification. An alternative to the penalty function is the penalty-and-reward function in which keystrokes incur either a penalty or a reward (i.e., a negative penalty) [5].

TABLE 4: User-dependent equal error rates. Bold indicates systems that are not significantly worse than the best system.

	Manhattan	Manhattan (scaled)	SVM (one-class)	HMM	POHMM
Password	0.088 (0.069)	0.062 (0.064)	0.112 (0.088)	0.126 (0.099)	0.042 (0.051)
Keypad	0.092 (0.069)	0.053 (0.030)	0.110 (0.054)	0.099 (0.050)	0.053 (0.025)
Mobile (w/o sensors)	0.194 (0.101)	0.097 (0.057)	0.170 (0.092)	0.168 (0.085)	0.090 (0.054)
Mobile (w/ sensors)	0.084 (0.061)	0.009 (0.027)	0.014 (0.033)	0.013 (0.021)	0.006 (0.014)
Fixed-text	0.085 (0.091)	0.049 (0.060)	0.099 (0.106)	0.105 (0.092)	0.031 (0.077)
Free-text	0.061 (0.092)	0.028 (0.052)	0.098 (0.091)	0.145 (0.107)	0.020 (0.046)

In this work, the sliding window replaces the reward since penalties outside the window do not contribute towards the cumulative penalty.

The penalty of each new event is determined as follows. The marginal probability of each new event, given the preceding events, is obtained from the forward lattice, α , given by

$$P(\mathbf{x}_{t+1}|\mathbf{x}_1^t) = P(\mathbf{x}_1^{t+1}) - P(\mathbf{x}_1^t) \quad (48)$$

When a new event is observed, the likelihood is obtained under every user’s model in a population of U models. The likelihoods are ranked, with the highest model given a rank of 0, and the lowest a rank of $U - 1$. The rank of the claimed user’s model is the incurred penalty. Thus, if a single event is correctly matched to the genuine user’s model, a penalty of 0 is incurred. If it scores the second highest likelihood, a penalty of 1 is incurred, and so on. The rank penalty is added to the cumulative penalty in the sliding window, while penalties outside the window are discarded.

Continuous verification performance is reported as the number of events that can occur before an impostor is detected. This is determined by increasing the penalty threshold until the genuine user is never locked out of the system. Since the genuine user’s penalty is always below the threshold, this is the maximum number of events that an impostor can execute before being rejected by the system while the genuine user is never rejected. If the impostor’s penalty never exceeds the threshold, then this is the entire length of the sample.

An example of the penalty function for genuine and impostor users is shown in Figure 9. The decision threshold is set to the maximum penalty incurred by the genuine user so that a false rejection does not occur. The average penalty for impostor users with 95% confidence interval is shown. In this example, the impostor penalties exceed the decision threshold after 81 keystrokes on average. Note that this is different than the average impostor penalty, which exceeds the threshold after 23 keystrokes.

For each dataset, the average maximum rejection time (AMRT) is determined, shown in Table 5. The maximum rejection time (MRT) is the maximum number of keystrokes needed to detect an impostor without rejecting the genuine user. The MRT is determined for each combination of impostor query sample and user model in the dataset to get the AMRT.

6 RELATED WORK

There have been various generalizations of the standard HMM (Figure 10) to deal with hidden states that are partially observable in some way. These models are referred to

TABLE 5: Continuous verification results.

	HMM	POHMM
Password	5.64 (2.04)	3.42 (2.04)
Keypad	4.54 (2.09)	3.45 (1.73)
Mobile (w/o sensors)	5.63 (2.18)	4.29 (2.02)
Mobile (w/ sensors)	0.15 (0.65)	0.12 (0.57)
Fixed-text	33.63 (15.47)	20.81 (9.07)
Free-text	129.36 (95.45)	55.18 (68.31)

as partly-HMM [14], partially-HMM [20], and context-HMM [9]. For clarity, these models have been redrawn in Figure 10 using the notation of this paper.

The partly-HMM (Figure 10a) is a second order model in which the first state is hidden and the second state is observable [14]. In the partly-HMM, both the hidden state and observation at time t_n are dependent on the observation at time t_{n-1} . The partly-HMM can be applied to problems that have a transient underlying process, such as gesture and speech recognition, as opposed to a piecewise stationary process that the HMM assumes [10]. Parameter estimation can be performed by expectation maximization (EM), similar to the HMM.

Partially observable states can also come in the form of partial and uncertain ground truth regarding the hidden state at each time step. The partially-HMM (Figure 10b) deals with this scenario, in which an uncertain hidden state label may be observed at each time step [20]. The probability of observing the uncertain label and the probability of the label being correct, were the true hidden state known, are controlled by parameters p_{obs} and p_{true} , respectively. Thus, the probability of observing a correct label is $p_{obs} \times p_{true}$. This model is motivated by language modeling applications in which manually labeling data is expensive and time consuming. Ground truth state labels may help in parameter estimation although they may be incorrect or missing due to human error [17]. Similar to the HMM, the EM algorithm can be used for estimating the parameters of the partially-HMM [20].

Past observations can also provide context for the transition and emission probabilities in a HMM. In [9], Forchhammer proposed the context-HMM, in which the transition and emission probabilities at time t are conditioned on an observed context function. The context functions are defined as $A_V(x_t) = v_t$ and $B_W(x_{t-1}) = w_t$ for the transition and emission probabilities, respectively, where the context sequences v_t and w_t are functions of the observation sequence. At each time step, the hidden state and observation are dependent on the context from the previous time step, shown

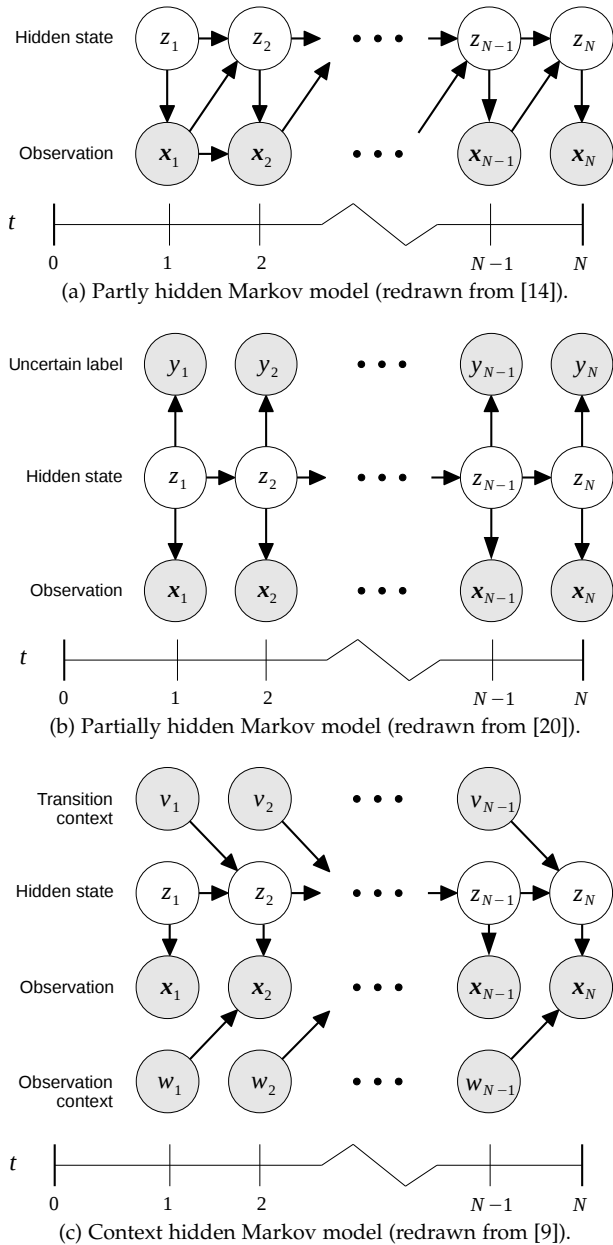


Fig. 10: Hidden Markov model generalizations for partially hidden states.

in Figure 10c. The context-HMM has information theoretic motivations, with applications such as image compression [8]. Used in this way, the neighboring pixels in an image can provide context for the emission and transition probabilities.

7 DISCUSSION

There are two scenarios in which previous models of partial observability fall short. The first is when there is missing data during parameter estimation, such as missing context, and the second is when there is missing or novel data during likelihood calculation. A possible solution to these problems uses the explicit marginal emission and transition distributions, where, e.g., the context is marginalized out. The model proposed in this work, described in Section 3, has explicit marginal distributions that act as a fallback

mechanism when observations with missing partial states are encountered. This leads directly to a parameter smoothing technique that restricts overfitting and allows the model to be applied to sequences with very few observations that would otherwise lead to degenerate distributions.

The POHMM is different from the partly-HMM [14], being a first order model, and different from the partially-HMM [20], since it doesn't assume a partial labeling. In particular, the POHMM makes the following assumptions.

- 1) There is some additional information associated with each event, such as an event type.
- 2) The event types form an independent Markov chain.
- 3) Some events have missing or unknown types.
- 4) Novel event types may be observed during likelihood calculation.

The POHMM is most similar to the context-HMM [9] in the sense that emission and transition probabilities are conditioned on some observed values. There are several important differences between the POHMM and context-HMM. In the POHMM, the hidden state at time t_n is dependent on event types at times t_n and t_{n-1} , whereas the hidden state of the context-HMM at time t_n is dependent only on the context at time t_{n-1} . Additionally, the context sequences are defined as functions of the observed values, which differ from the event types of the POHMM. For missing event types, the marginal distributions of the POHMM also act as a fallback mechanism, whereas the context-HMM cannot account for missing or unknown context. This is an important distinction since novel event type sequences may be observed during testing. The marginal distributions of the POHMM are also used in parameter smoothing, which reduces the *dof* of the model and provides superior parameter estimates with small amounts of data.

8 CONCLUSION

This work introduced the POHMM, an extension of the HMM in which hidden states are partially observable through event types. A subclass of the POHMM is the HMM in which the event types are all the same or unknown. The POHMM marginal distributions can account for missing data during testing, while parameter smoothing helps to avoid overfitting and accounts for missing data during training. Model consistency was demonstrated empirically and analytically, and the estimated parameter residuals were shown to be lower when a parameter smoothing strategy is employed. Computational complexities of the POHMM parameter estimation and likelihood calculation algorithms are comparable to that of the HMM, which are linear in the number of observations.

The application of the POHMM extends beyond keystroke biometrics, and the two-state model of temporal behavior proposed in this work can be used for other types of time intervals. There are a number of reasons to utilize time intervals as a behavioral biometric. Timestamped events from human behavior are truly ubiquitous. In the Information Age, most human-computer interactions generate timestamped events in some way. From the keys pressed on a keyboard and the transmission of an email message, to the submission of a research article through an online

submission system, a timestamp is generated and stored for each event. In many scenarios, timestamps can be observed without user cooperation or knowledge, further increasing the ubiquity of human temporal behavior.

REFERENCES

- [1] Ned Bakelman, John V Monaco, Sung-Hyuk Cha, and Charles C Tappert. Keystroke biometric studies on password and numeric keypad input. In *European Intelligence and Security Informatics Conference (EISIC)*, pages 204–207. IEEE, 2013.
- [2] A-L Barabási, K-I Goh, and A Vazquez. Reply to comment on “the origin of bursts and heavy tails in human dynamics”. *arXiv preprint physics/0511186*, 2005.
- [3] Albert-Laszlo Barabási. The origin of bursts and heavy tails in human dynamics. *Nature*, 435(7039):207–211, 2005.
- [4] Norbert Blenn and Piet Van Mieghem. Are human interactivity times lognormal? *arXiv preprint arXiv:1607.02952*, 2016.
- [5] Patrick Bours. Continuous keystroke dynamics: A different perspective towards biometric evaluation. *Information Security Technical Report*, 17(1):36–43, 2012.
- [6] Patrick Bours and Soumik Mondal. Performance evaluation of continuous authentication systems. *IET Biometrics*, 2015.
- [7] Christophe Couvreur. *Hidden Markov models and their mixtures*. DEA Report, Dep. of Mathematics, Université catholique de Louvain, 1996.
- [8] Søren Forchhammer and Tage S Rasmussen. Adaptive partially hidden markov models with application to bilevel image coding. *Image Processing, IEEE Transactions on*, 8(11):1516–1526, 1999.
- [9] Søren Otto Forchhammer and Jorma Rissanen. Partially hidden markov models. *IEEE Transactions on Information Theory*, 42(4):1253–1256, 1996.
- [10] T Iobayashi, Junko Furuyama, and Ken Mas. Partly hidden markov model and its application to speech recognition. In *Acoustics, Speech, and Signal Processing, 1999. Proceedings., 1999 IEEE International Conference on*, volume 1, pages 121–124. IEEE, 1999.
- [11] L Jain, JV Monaco, MJ Coakley, and CC Tappert. Passcode keystroke biometric performance on smartphone touchscreens is superior to that on hardware keyboards. *International Journal of Research in Computer Applications & Information Technology*, 2(4):29–33, 2014.
- [12] Dan Jurafsky, James H Martin, Andrew Kehler, Keith Vander Linden, and Nigel Ward. *Speech and language processing: An introduction to natural language processing, computational linguistics, and speech recognition*, volume 2. MIT Press, 2000.
- [13] Kevin S Killourhy and Roy A Maxion. Comparing anomaly-detection algorithms for keystroke dynamics. In *Dependable Systems & Networks, 2009. DSN’09. IEEE/IFIP International Conference on*, pages 125–134. IEEE, 2009.
- [14] Tetsunori Kobayashi and Satoshi Haruyama. Partly-hidden markov model and its application to gesture recognition. In *Acoustics, Speech, and Signal Processing, 1997. ICASSP-97., 1997 IEEE International Conference on*, volume 4, pages 3081–3084. IEEE, 1997.
- [15] Yi Lu and Leilei Zeng. A nonhomogeneous poisson hidden markov model for claim counts. *Astin Bulletin*, 42(01):181–202, 2012.
- [16] R Dean Malmgren, Daniel B Stouffer, Adilson E Motter, and Luís AN Amaral. A poissonian explanation for heavy tails in e-mail communication. *Proceedings of the National Academy of Sciences*, 105(47):18153–18158, 2008.
- [17] Bernard Merialdo. Tagging english text with a probabilistic model. *Computational linguistics*, 20(2):155–171, 1994.
- [18] John V Monaco, Ned Bakelman, Sung-Hyuk Cha, and Charles C Tappert. Recent advances in the development of a long-text-input keystroke biometric authentication system for arbitrary text input. In *European Intelligence and Security Informatics Conference (EISIC)*, pages 60–66. IEEE, 2013.
- [19] Whitney K Newey and Daniel McFadden. Large sample estimation and hypothesis testing. *Handbook of econometrics*, 4:2111–2245, 1994.
- [20] Huseyin Ozkan, Arda Akman, and Suleyman S Kozat. A novel and robust parameter training approach for hmms under noisy and partial access to states. *Signal Processing*, 94:490–497, 2014.
- [21] Lawrence Rabiner. A tutorial on hidden markov models and selected applications in speech recognition. *Proceedings of the IEEE*, 77(2):257–286, 1989.
- [22] Vasanthan Raghavan, Aram Galstyan, Alexander G Tartakovsky, et al. Hidden markov models for the activity profile of terrorist groups. *The Annals of Applied Statistics*, 7(4):2402–2430, 2013.
- [23] Ricardo N Rodrigues, Glauco FG Yared, Carlos R do N Costa, João BT Yabu-Uti, Fábio Violaro, and Lee Luan Ling. Biometric access control through numerical keyboards based on keystroke dynamics. In *Advances in Biometrics*, pages 640–646. Springer, 2005.
- [24] G Rupert Jr et al. *Simultaneous statistical inference*. Springer Science & Business Media, 2012.
- [25] Timothy A Salthouse. Perceptual, cognitive, and motoric aspects of transcription typing. *Psychological bulletin*, 99(3):303, 1986.
- [26] DB Stouffer, RD Malmgren, and LAN Amaral. Comments on “the origin of bursts and heavy tails in human dynamics”. *arXiv preprint physics/0510216*, 2005.
- [27] RL Stratonovich. Conditional markov processes. *Theory of Probability & Its Applications*, 5(2):156–178, 1960.
- [28] Charles C Tappert, Sung-Hyuk Cha, Mary Villani, and Robert S Zack. A keystroke biometric system for long-text input. *International Journal of Information Security and Privacy (IJISP)*, 4(1):32–60, 2010.
- [29] Charles C Tappert, Mary Villani, and Sung-Hyuk Cha. Keystroke biometric identification and authentication on long-text input. *Behavioral biometrics for human identification: Intelligent applications*, pages 342–367, 2009.
- [30] Mary Villani, Charles Tappert, Giang Ngo, Justin Simone, H St Fort, and Sung-Hyuk Cha. Keystroke biometric recognition studies on long-text input under ideal and application-oriented conditions. In *Computer Vision and Pattern Recognition Workshop, 2006. CVPRW’06. Conference on*, pages 39–39. IEEE, 2006.



John V. Monaco is a Postdoctoral Fellow at the Computational and Information Sciences Directorate of the U.S. Army Research Laboratory and Adjunct Professor at Pace University. Dr. Monaco earned his BS in Computer Science and Mathematics (2012), MS in Computer Science (2013), and Ph.D in Computer Science (2015) from Pace University. In 2011, he was selected for the highly competitive and prestigious Information Assurance Scholarship Program by the U.S. Department of Defense. In 2013, Dr. Monaco was named one of Westchester’s “Top Professionals under 30” for research in keystroke biometrics at Pace University. He has since achieved first place in several international biometric competitions. His primary areas of interest are behavioral biometrics, machine learning, and neuromorphic computing.

Charles C. Tappert is a Professor of computer science and Associate Program Director of the Doctor of Professional Studies (D.P.S.) in computing program at Pace University. He received his B.S. degree from Swarthmore College in PA, and M.S. and Ph.D. from Cornell University, Ithaca, NY. He joined IBM in 1967 and has been a Research Staff Member of the IBM T. J. Watson Research Center, Yorktown Heights, NY since 1972. His research has primarily been in the area of pattern recognition. He worked on automatic speech recognition and speech coding for ten years. Since 1978 he has been working on tablet terminals, where his main interest has been computer recognition of hand printing and cursive writing. He has extensive experience in computer science, specializing in pattern recognition, pen computing and speech applications, information assurance, e-commerce, and artificial intelligence. Dr. Tappert has taught graduate and undergraduate courses, supervised dissertations, secured government contracts, and has over 100 publications including book chapters, journal articles, conference papers, and patents.